Appl. Phys. B 79, 153–162 (2004)
DOI: 10.1007/s00340-004-1547-x

Applied Physics B
Lasers and Optics

R. PASCHOTTA

Noise of mode-locked lasers (Part I): numerical model

Ultrafast Laser Physics, Institute of Quantum Electronics, Swiss Federal Institute of Technology, ETH Hönggerberg HPT, 8093 Zürich, Switzerland

Received: 19 February 2004/Revised version: 22 April 2004
Published online: 31 May 2004 •

ABSTRACT A numerical model for the calculation of noise spectra of actively or passively mode-locked lasers has been developed. Fluctuations not only of the timing error, but also of all other quantities of interest can be quantified. The model is based on a pulse propagation algorithm with quantum noise sources. It allows the study of a much wider class of phenomena than those accessible with analytical techniques, and it is useful for testing the validity limits of analytical results.

PACS 43.50.+y, 42.50.Lc, 42.60.Fc

1 Introduction

Mode-locked lasers generate trains of quite regularly spaced optical pulses, which are useful for a very wide class of applications. The noise properties of the pulse trains are of interest as a subject of fundamental physics as well as for applications. In particular, the timing jitter can affect optical data transmission, optical sampling measurements, and experiments with synchronized lasers. Noise also occurs in other quantities such as the pulse energy, pulse duration, chirp, optical phase, etc. In a laser, these types of noise are coupled to each other in various ways, depending on the circumstances.

A quantitative understanding of laser noise is highly desirable from a theoretical perspective as well as a prerequisite for systematic minimization of noise by proper laser design. In recent years, some analytical models [1–3] have generated significant insight. In particular, the model by Haus and Mecozzi [2] describes the noise of lasers which are passively mode-locked with a fast saturable absorber and which have soliton-like pulses circulating in the resonator, while Hjelme et al. [1] treated actively mode-locked lasers. However, all such analytical models become rather sophisticated while remaining restricted to rather limited situations. For example, such limitations concern mode locking with slow saturable absorbers, e.g. semiconductor saturable absorber mirrors (SESAMs, [4, 5]), and also the realistic modeling of intensity noise and its coupling to timing noise in various ways, and the noise in other quantities such as the pulse duration, which may be coupled to timing noise.

✉ Fax: +41-1/6331059, E-mail: paschotta@phys.ethz.ch

A comprehensive discussion of the noise properties of mode-locked lasers thus requires a combination of analytical and numerical techniques. In this paper, which forms part one of a two part article, I describe in detail a numerical model, which allows calculation of the noise properties of a very wide class of actively or passively mode-locked lasers. Here, mode locking can be achieved by using a modulator, a fast or slow saturable absorber, or even by a combination of these. The results of the numerical model have been compared with analytical results in simple cases, but have also been used in cases which can not be treated with existing analytical models, such as cases with realistic gain saturation, where relaxation oscillations occur and couple to the timing fluctuations via various effects, such as temporal shifts introduced by a slow saturable absorber, a Kerr nonlinearity with self-steepening in the gain medium, or phase profiles of the gain medium obtained via Kramers–Krönig relations. This leads in part to surprising, although physically explainable results, as discussed in the second part [6] of this article. For example, I found that the coupling between intensity and timing noise in a slow saturable absorber can be eliminated by correctly adjusting the degree of saturation.

To my knowledge, the literature so far contains only a short mention of a similar numerical model [7], but no detailed description or even a detailed discussion of results. While the general approach of numerical modeling is quite straight-forward, there are a couple of non-trivial problems to be solved in order to obtain reliable numerical results. In the following, this is discussed in detail. After correction of some trivial errors in the Haus/Mecozzi calculations [2], the results of their analytical model agree with the numerical model not only for soliton mode-locked lasers with a fast saturable absorber, but also for lasers without any dispersion and nonlinearity, even though this situation is clearly outside the assumptions underlying the analytical model. Alternative derivations of the key results, which do not depend on soliton perturbation theory, allows to explain this finding in part two of this article [6].

2 Definitions for the characterization of noise

Unfortunately, the literature on noise in lasers suffers from a confusion which largely arises from different conventions, frequently incomplete specification of conventions,

and also partly from mathematical difficulties. Examples are the use of one-sided and two-sided power densities, and the relations between timing noise, phase noise, and the noise observed in the radio-frequency spectrum of a photodiode, particularly under conditions of large phase noise where first-order approximations break down. In the following I attempt to clearly explain the notation and a few basic mathematical aspects for use in both parts of this article.

This article deals with the noise in several parameters of the pulses generated by mode-locked lasers. It is always assumed that the pulses are completely separable from each other, which is normally the case in existing lasers. Of particular interest is the timing error Δt, which is the deviation of the temporal position of a pulse from a reference, which can be chosen to be the corresponding pulse position for a hypothetical laser without any noise inputs. More precisely, the temporal position t_p is not defined by the power maximum but rather by the "center of gravity":

$$t_\mathrm{p} \equiv \frac{\int t\ P(t)\ \mathrm{d}t}{\int P(t)\ \mathrm{d}t} \tag{1}$$

with the optical power $P(t)$. The integration range should fully cover one pulse, but not overlap with neighboring pulses.

The timing error Δt is frequently transformed into a phase error

$$\Delta\varphi = 2\pi f_\mathrm{rep} \times \Delta t\,, \tag{2}$$

(where f_rep is the pulse repetition rate) so that the timing noise is often called phase noise. This is the phase noise of the lowest harmonic of the output of a photodiode detecting the power of the pulse train. In order to avoid confusion with the noise in the optical phase of the pulses, the term timing phase noise is used for this.

Other pulse parameters of interest are the pulse energy E_p, the FWHM (full width at half maximum) pulse duration τ_p, the deviation Δf_c of the optical center frequency from the reference frequency f_ref, and the optical phase φ_opt.

The noise in all these pulse parameters can be quantified by two-sided spectral power densities. For example, there is the power density $S_\varphi(f)$ corresponding to the timing phase φ. Note that spectral power densities of such quantities which do not vanish for large times can not be simply defined as the squared modulus of the Fourier transform, as the corresponding integrals would diverge. One possibility is to remove the divergence with a definition like

$$S_\varphi(f) \equiv \lim_{T\to\infty} \frac{1}{T} \left| \int_{-T/2}^{+T/2} \Delta\varphi(t)\ \mathrm{e}^{+\mathrm{i}2\pi ft} \mathrm{d}t \right|^2 , \tag{3}$$

where the Fourier transform is calculated for a finite time interval of width T and the limit for $T \to \infty$ is used. The Wiener–Khinchin theorem states that this definition is equivalent to

$$S_\varphi(f) = \int_{-\infty}^{+\infty} G_\varphi(\tau)\ \mathrm{e}^{\mathrm{i}2\pi f\tau} \mathrm{d}\tau, \tag{4}$$

with the autocorrelation function

$$G_\varphi(\tau) = \langle \Delta\varphi(t)\Delta\varphi(t+\tau)\rangle\,, \tag{5}$$

where $\langle ...\rangle$ denotes an expectation value (ensemble average). In fact, (4) is often the simplest way of obtaining noise spectra in analytical calculations, while numerical calculations are usually based on the squared modulus of the Fourier transform of the data for a finite time span T, divided by T. In any case, the units of $S_\varphi(f)$ are $\mathrm{rad}^2\,\mathrm{s} = \mathrm{rad}^2/\mathrm{Hz}$, while the units of the Fourier transform would be $\mathrm{rad}^2\,\mathrm{s}^2$.

Note that these are two-sided spectral densities, defined for both positive and negative frequencies. As the quantities of interest are all real, $S(-f) = S(f)$ for all these quantities. The corresponding one-sided spectral densities (which are more common in the engineering disciplines), defined only for non-negative frequencies, are just two times higher.

Using (5), one can calculate the variance according to

$$\sigma_{\Delta\varphi}^2 \equiv \langle |\Delta\varphi|^2\rangle = \int_{-\infty}^{+\infty} S_\varphi(f)\ \mathrm{d}f\,, \tag{6}$$

although such integrals are not always convergent. For example, the integral would diverge for a free-running passively mode-locked laser due to the divergence of $S_\varphi(f)$ at $f = 0$.

In other articles, spectral densities are often used as functions of the angular frequency $\omega = 2\pi f$. Confusion then often arises from different normalization. Some authors adjust the normalization of spectral densities so that (6) simply reads with ω instead of f; the ω-dependent spectral densities are then lower by a factor of 2π to compensate for the larger differential $\mathrm{d}\omega = 2\pi\ \mathrm{d}f$. Other authors, such as Haus et al. [2], write all frequency integrals with the differential $\mathrm{d}\omega/2\pi$, so that their spectral densities have the same magnitude as those with the variable f, are used throughout this article. Additional problems of this type can arise when the noise of frequency variables, such as the repetition frequency f_rep or $\omega_\mathrm{rep} = 2\pi f_\mathrm{rep}$, are considered.

When the power of the pulse train is detected with a photodiode, the spectrum of the resulting photodiode signal has a significant spectral power density near the harmonics of the repetition frequency, and this spectrum is related to the timing phase noise. However, this relation is not trivial. First of all, intensity noise also affects this spectrum. The effects of intensity and phase noise on this spectrum can, under certain circumstances, be distinguished from each other by comparing the noise sidebands of several harmonics ([8–11]). In simple cases where the intensity noise is negligible and the phase excursion stays small (i.e., $|\Delta\varphi| \ll 1$ for all times), a simple relation is obtained. One typically describes the photodiode signal around the first harmonic at $f = f_\mathrm{rep}$ with a normalized power density $L(f)$, where f is the noise frequency (deviation from f_rep) and the integral of $L(f)$ over the first harmonic is unity. With $L(f) = \Delta(f) + L_\mathrm{noise}(f)$, where $\Delta(f)$ is the Dirac delta function and the power contribution of $L_\mathrm{noise}(f)$ to the integral of $L(f)$ is usually very small compared to the contribution of the delta function. With $|\Delta\varphi| \ll 1$ for all times (which is usually the case in actively mode-locked lasers or in timing-stabilized passively mode-locked lasers), and assuming weak noise in the intensity and other parameters, this

gives $L_{\text{noise}}(f) = S_\varphi(f)$, if $S_\varphi(f)$ is two-sided (or one half this value for one-sided $S_\varphi(f)$). This means

$$L(f) = \delta(f) + S_\varphi(f)\,. \tag{7}$$

However, note that this simple relation does not hold for large phase excursion, which can easily occur in free-running passively mode-locked lasers. In that case, the spectral density of the photodiode signal has a finite value at $f = f_{\text{rep}}$ while $S_\varphi(f)$ is divergent at $f = 0$. For example, a Lorentzian form of $L(f)$ is obtained for cases with $S_\varphi(f) \propto f^{-2}$.

Note that in order to avoid this kind of complication, the revised IEEE standard 1139-1988 [12] uses the definition $L(f) \equiv S_\varphi(f)$ (adapted to the notation with two-sided $S_\varphi(f)$) even for large phase excursions. However, $L(f)$ then no longer corresponds to the measured photodiode spectrum.

The timing noise can alternatively be characterized by the noise of the instantaneous repetition rate, defined as the inverse spacing of subsequent pulses. The power densities are related to each other by

$$S_\varphi(f) = \frac{1}{f^2} S_{f_{\text{rep}}}(f)\,, \tag{8}$$

where f is the noise frequency. This shows that for example white noise in the repetition frequency corresponds to f^{-2} noise in the timing phase or in the timing error Δt, i.e., slower frequency fluctuations lead to larger accumulated timing deviations.

For most other pulse parameters, I prefer to use the spectral power densities of normalized quantities. In particular, I use the intensity noise $S_I(f)$ corresponding to the spectrum of the pulse energy divided by its average value, and accordingly $S_\tau(f)$ for the spectrum of the normalized pulse duration and $S_{\Delta f_c}(f)$ for the normalized center frequency. Only for the optical phase φ_{opt} such a normalization is not required.

3 Pulse propagation with quantum noise sources

The basic principle of this model is to numerically propagate a pulse through the laser cavity, taking into account influences from all intracavity elements, in particular from the gain medium, linear and nonlinear losses, dispersion, and nonlinearities. Various noise sources can be included in the propagation. The pulse properties like pulse energy, temporal position, duration, etc. are recorded after each cavity round-trip (or only after each tenth round-trip). Finally, the results are statistically processed in order to obtain noise spectra.

3.1 *Representation of the pulses*

3.1.1 Continuous functions. In an analytical model, the state of a pulse can be described by a complex envelope $A(t)$ in the time domain, or by a complex envelope $A(f)$ in the frequency domain. These functions are considered to only describe a single pulse, and not a pulse train.

The complex amplitude (envelope) $A(t)$ is normalized so that the power is

$$P(t) = |A(t)|^2\,. \tag{9}$$

The "E field" is defined as

$$E(t) = \text{Re}\left(A(t)\exp(-\text{i}2\pi f_{\text{ref}} t)\right), \tag{10}$$

and does not have the units of an electric field but rather the units $\sqrt{\text{W}}$. The fast optical oscillation is removed from the amplitude function by introducing the reference frequency f_{ref}, which is normally chosen to be close to the center frequency of the pulse. The envelope $A(t)$ is then only slowly varying, i.e., on time scales larger than the optical oscillation period, particularly for long pulses.

In the frequency domain, there is the complex envelope $A(f)$. Time and frequency domains are related by Fourier transforms:

$$A(t) = \int_{-\infty}^{+\infty} A(f) \times \exp(-\text{i}2\pi f t)\,\text{d}f \tag{11}$$

$$A(f) = \int_{-\infty}^{+\infty} A(t) \times \exp(+\text{i}2\pi f t)\,\text{d}t \tag{12}$$

As the temporal amplitude does not contain the fast optical oscillation, the frequency domain amplitudes correspond not to optical frequencies but to frequency offsets f relative to f_{ref}.

A positive phase shift applied to the complex amplitude $A(t)$ means a phase delay, while a negative phase shift means an advance of the phase.

The pulse energy is

$$E = \int_{-\infty}^{+\infty} |A(t)|^2\,\text{d}t = \int_{-\infty}^{+\infty} |A(f)|^2\,\text{d}f\,. \tag{13}$$

3.1.2 Numerical representation. In the numerical model, the envelope functions $A(t)$ and $A(f)$ of a pulse are represented by one-dimensional arrays A_j and $\tilde{A}_j$ of complex values with an integer index j running from 1 to N, the total number of points, which should be a power of 2. In this case, the simplest form of a Fast Fourier Transform (FFT) algorithm can be used to switch between time and frequency domain.

The temporal samples A_j (with units $\sqrt{W}$) are located symmetrically around $t = 0$. More precisely, $t = 0$ corresponds to $j = j_0 \equiv N/2$, and the index j corresponds to $t_j = (j - j_0)\delta t$ with the temporal resolution δt. This means that the time span ranges from $(1 - j_0)\delta t$ to $(N - j_0)\delta t$. Although $t_N - t_1 = (N - 1)\delta t$, the temporal samples can be interpreted to represent a temporal range of $T = N\,\delta t$ as each sample represents a time interval of width δt around $t_j = (j - j_0)\delta t$.

The temporal resolution δt is usually chosen so that the main part of the pulse is covered with ≈ 20 samples. The whole trace typically contains 256 or 512 samples, i.e., it spans a range in the order of 20–40 pulse durations. As discussed in Sect. 4.1, this relatively course sampling is sufficient. Also note that particularly for lasers with low repetition rates, the represented time span is typically chosen to be only a small fraction of the pulse repetition period, because there is negligible power outside this time span. Note, however, that for lasers with high repetition rates, or more precisely,

for lasers where the pulse duration is not orders of magnitude smaller than the repetition period, it can become necessary to make the length of the represented time span identical to the repetition period, if some interaction of adjacent pulses occurs through the pulse wings.

In the frequency domain, the pulse is represented by complex amplitudes $\tilde{A}_j$, corresponding to the discrete offset frequencies $f_j = (j - j_0)\,\delta f$ relative to the reference frequency f_{ref}. The frequency resolution is $\delta f = 1/T$ and the width of the frequency range $F = N\delta f = N/T$. The units of $\tilde{A}_j$ are $\sqrt{\mathrm{J}}/\sqrt{\mathrm{Hz}}$, and $\left|\tilde{A}_j\right|^2$ is the power of a frequency bin with units J/Hz. The maximum frequency offset is $(N/2)\delta f = N/2T$ (the Nyquist frequency).

The total pulse energy is then

$$E_{\mathrm{p}} = \delta t \sum_{j=1}^{N} \left|A_j\right|^2 = \delta f \sum_{j=1}^{N} \left|\tilde{A}_j\right|^2. \tag{14}$$

3.2 *Object-oriented approach*

The object-oriented programming approach, which I have used in the development platform Borland Delphi, is highly convenient for such modeling. Here, each pulse is represented as an object, holding the time and frequency traces as dependent objects. Numerous methods of the pulse object have been implemented to do certain operations on a pulse or to deliver pulse qualities such as energy, duration, or spectral power densities. The laser cavity is another object, holding dependent objects which represent all optical elements, which themselves can act on pulse objects. These actions are executed by one or several operators, representing effects like laser gain, nonlinearity, or dispersion. Depending on the particular case, an operator may act in the time domain or in the frequency domain, providing the representation of the modified pulse in one domain and invalidating the trace of the other domain. The latter can later be obtained by applying the FFT algorithm, if required.

3.3 *Pulse propagation without quantum noise*

The effect of intracavity optical elements on the pulse are all reflected by certain changes of the amplitude given either in the time or frequency domain. In the following I briefly summarize only the most important operations, as other effects and extensions are relatively straight-forward to implement. Depending on the type of laser, a suitable combination of optical elements (in the case of my program described by commands in an input text file) are used in the model. For example, in a standing-wave cavity the gain medium may appear twice (for both directions of travel), although both passages through the gain medium can often be combined into a single one for simplicity.

3.3.1 Laser gain. The application of a constant gain corresponding to a power amplification factor G is trivial, it simply amounts to a multiplication of all amplitudes in the time or frequency domain with $\sqrt{G}$. A simple extension is wavelength-dependent gain, which is applied preferentially in the frequency domain, making the applied factor frequency-dependent. In this case, it is possible to take into account the phase profile associated with the gain, which can be calculated for arbitrary gain profiles using Kramers–Krönig relations (adapted from [13]):

$$\Delta\varphi(\nu) = -\frac{\nu}{\pi}\wp \int_0^{+\infty} \frac{\ln G(\nu')}{\nu'^2 - \nu^2}\mathrm{d}\nu', \tag{15}$$

where $\Delta\varphi$ is the spectral phase change and $G(\nu)$ is the power amplification factor at the optical frequency ν, while $\wp$ stands for the principle value of the integral. Such a phase profile contributes some amount of dispersion, which can be simply added to other contributions of dispersion in the cavity. More importantly, the gain can fluctuate, and the Kramers–Krönig phase profile translates these fluctuations into noise of the optical phase and of the timing. The Haus/Mecozzi model [2], incorporated a term which can describe such effects for a simple Lorentzian gain spectrum, although this term has later been dropped in the calculation of the timing jitter, apparently because it is negligible in the particular case of a Ti:sapphire laser.

Another essential property of laser gain is that it can be saturated. The Haus/Mecozzi model uses a very simple type of gain saturation, depending on the pulse energy but not on its history. This may be a reasonable approximation for semiconductor lasers, where the gain very quickly responds to changes of pulse energy, but not for typical solid-state lasers, where gain saturation accumulates over many round-trips, leading to phenomena such as relaxation oscillations. A realistic model of these, making possible a study of timing noise arising from intensity fluctuations, must be based on a dynamical variable for the gain which evolves together with the pulse according to a differential equation of the form

$$\frac{\partial}{\partial t} g = -\frac{g - g_{\mathrm{ss}}}{\tau_{\mathrm{g}}} - \frac{g\,P}{E_{\mathrm{sat,g}}}, \tag{16}$$

(valid for $|g| \ll 1$) where g is the gain coefficient (corresponding to a power amplification factor $G = \exp(g)$), g_{ss} is the steady-state small-signal gain, τ_{g} is the gain recovery time (spontaneous lifetime of upper laser level), P is the intracavity laser power (averaged over one cavity round-trip), and $E_{\mathrm{sat,g}}$ the saturation energy of the gain.

In solid-state lasers, the pulse energy is normally well below $E_{\mathrm{sat,g}}$, so that the gain g has to be numerically updated only once per round-trip, but not during a pulse. This also allows application of the gain in the frequency domain, so that it can be made frequency-dependent. For broad pulse spectra (extending significantly beyond the spectral gain maximum), one may then use an effective saturation energy depending on the pulse spectrum.

In solid-state lasers, the gain saturation may be homogeneous or inhomogeneous, but as long as the pulse energy stays well below the saturation energy, the type of gain saturation is of limited importance. It is only that inhomogeneous saturation will distort the shape of the saturated gain spectrum, but this shape will be nearly constant for given parameters of the laser and can easily be incorporated in the numerical model. Only for the rare case of a laser with strong saturation

during a pulse will inhomogeneous saturation make a more complicated model necessary, where the gain medium is decomposed into a series of frequency components with independent interaction with the optical field.

Finally, gain and intensity fluctuations are often excited by pump noise. Nowadays, diode lasers, often in the form of diode bars, are commonly used as pump sources. Although diode lasers do not exhibit the very large low-intensity noise originating in arc lamps, their noise is usually 20–30 dB above the shot noise level for diode bars, or about 10 dB above the shot noise level for single-element diode lasers [14], which can however, provide only a few hundred milliwatts of pump power. At frequencies up to the relaxation oscillation frequency, this pump noise induces a large excess noise in the intensity of the mode-locked laser, and this can affect the timing noise as well.

The pump noise can be quite easily incorporated into the model if one assumes a flat noise spectrum (i.e., white noise) for the pump laser, a pulse repetition rate far above the upper-state lifetime of the gain medium, and a four-level gain medium. These assumptions are reasonable for most mode-locked solid-state lasers pumped with diode bars. Then, within one pulse period the pump contributes an averaged value of

$$\Delta g = \frac{T_{\mathrm{rt}}}{\tau_{\mathrm{g}}} g_{\mathrm{ss}} \tag{17}$$

to the gain, where $T_{\mathrm{rt}} = 1/f_{\mathrm{rep}}$ is the round-trip time. (A smaller part of this change is lost by spontaneous emission.) This change of gain corresponds to contributing an average number

$$\Delta N = \Delta g \frac{E_{\mathrm{sat,g}}}{h\nu} = \frac{T_{\mathrm{rt}}}{\tau_{\mathrm{g}}} g_{\mathrm{ss}} \frac{E_{\mathrm{sat,g}}}{h\nu} \tag{18}$$

to the excited-state population. For a shot-noise-limited pump, the variance of this value equals its average value. The corresponding variance added to g is

$$\sigma_g^2 = \frac{h\nu}{E_{\mathrm{sat,g}}} g_{\mathrm{ss}} \frac{T_{\mathrm{rt}}}{\tau_{\mathrm{g}}}. \tag{19}$$

Thus, a random value with a Gaussian distribution and the calculated variance can just be added to the gain after each round-trip. If the pump noise power density is above the shot noise level by a certain factor, the variance of (19) can be multiplied by this factor.

For a pump source with a non-constant power density, one can generalize the procedure by adding noise amplitudes to the gain which are partially correlated to each other.

3.3.2 Saturable absorption. The case of a fast saturable absorber is the simpler one. Here, the loss is instantaneously reacting to the optical power:

$$l(t) = \frac{l_0}{1 + P(t)/P_{\mathrm{sat}}}, \tag{20}$$

with the unsaturated loss l_0 and a saturation power P_{sat}. The approximation of weak absorber saturation, as typically used in analytical models (although it is often not accurate), is not required.

A slow saturable absorber can be modeled with an equation similar to (16). However, there are usually significant changes of absorption occuring during the passage of the pulse, so that (16) has to be solved on this short time scale. This makes it difficult to include a frequency dependence of the saturable absorption.

The excitation of an absorber may also change the phase delay for the pulses. This effect is often described by the so-called linewidth enhancement factor α, which originally has been introduced in the context of semiconductor lasers [15] but can also be used for saturable absorbers. A numerical model even allows going beyond a simple linear relation between absorption and phase delay, but the assumption of a wavelength-independent saturable absorption is required to keep the equations reasonably simple.

3.3.3 Active modulator. The effect of an active modulator on the pulses can be described by a simple time-dependent amplitude transmission factor. In addition, in some cases there is also a significant change of the phase delay. In this case, a time-dependent complex transmission factor can be used.

3.3.4 Dispersion. While the Haus/Mecozzi model [2] contains only second-order dispersion, a numerical model allows treatment of the dispersion of arbitrary spectral shapes. No matter how the dispersion is specified, one can calculate an array of spectral phase shifts, used to rotate the complex phases of the pulse amplitudes in the frequency domain.

3.3.5 Kerr nonlinearity. The Kerr effect changes the refractive index of a material in proportion to the optical intensity. It results from the instantaneous nonlinear response of the material, which arises mainly from electronic polarization and is important in most mode-locked lasers. The phase change caused to the optical power P by the Kerr effect in a medium with nonlinear index n_2 and length L, where the Gaussian beam radius in the medium is w, can be calculated as

$$\Delta\varphi = \Delta n(I) \frac{2\pi}{\lambda} L = n_2 \frac{P}{\pi w^2/2} \frac{2\pi}{\lambda} L = \frac{4 n_2\, P\, L}{\lambda\, w^2}. \tag{21}$$

Note that the intensity used is the peak intensity of the Gaussian profile, rather than some averaged intensity. The phase change on the beam axis can be then obtained, while the reduction of the nonlinear phase change at other radial positions leads to Kerr lensing. The latter can be used for Kerr-lens mode locking [16], i.e., an effective fast saturable absorption effect arising from power-dependent mode sizes in the laser cavity. While a full spatio-temporal description of such effects is very difficult, one can approximately describe the Kerr lensing effect by adding a fast saturable absorber in the model.

A closer inspection of effects caused by nonlinear polarization reveals that (21) is only an approximation. Besides the nonlinear phase change, there is also a nonlinear change of the group velocity in the medium. This effect, called self-steepening [17], directly affects the temporal pulse position, and as this temporal shift depends on the pulse energy and duration, it leads to a coupling of noise in the intensity and pulse duration to timing noise. A comprehensive study of these kind of effects requires the implementation of the self-steepening

effect. Reference [18] presents an equation to describe the combined action of the ordinary Kerr effect and the self-steepening correction:

$$\frac{\partial}{\partial z}A(z,t) = \mathrm{i}\gamma\left(1+\frac{\mathrm{i}}{\omega_0}\frac{\partial}{\partial t}\right)\left(|A(z,t)|^2\,A(z,t)\right). \tag{22}$$

Here, $A(z,t)$ is a complex amplitude describing pulse propagation in a fiber along the z direction, and (22) shows only the nonlinear term with the coefficient $\gamma \propto n_2/w^2$. For a numerical implementation, the self-steepening term with the time derivative needs special attention. It is usually not advisable to approximate it with finite differences. Instead, one can use the fact that in the frequency domain the first parenthesis represents a multiplication with the optical angular frequency ω, divided by the mean frequency ω_0. One can therefore compute the Fourier transform of the right parenthesis, multiply the result with ω/ω_0, and then apply the inverse Fourier transform. Equation (22) demonstrates that the common approximation without the self-steepening term amounts to replacing the optical frequency with the optical mean frequency, which is often acceptable for narrow pulse spectra. For short pulses, however, the temporal shift caused by the self-steepening effect is more important, in particular because it often becomes strong due to the high peak intensities in femtosecond laser cavities.

3.4 *Quantum noise sources*

For numerical modeling of the influence of quantum noise, I use a semiclassical approach, namely the Wigner method [19]. Here, the complex amplitudes $A(t)$ and $\tilde{A}(t)$ in the time and frequency domain, respectively, carry quasi-classical random fluctuations which are excited by random noise terms arising from various interactions.

The initial pulse is usually assumed to have noise at the standard quantum noise level. This amounts to having a random noise amplitude $\delta A(t)$ in the time domain with an autocorrelation

$$G_{\delta A}(\tau) \equiv \langle \delta A^*(t)\;\delta A(t+\tau)\rangle = \frac{h\nu}{2}\delta(\tau), \tag{23}$$

where $h\nu$ is the photon energy. This noise is related to a two-sided power density

$$S_{\delta A}(f) = \int_{-\infty}^{+\infty} G_{\delta A}(t)\;\mathrm{e}^{\mathrm{i}2\pi ft}\;\mathrm{d}t = \frac{h\nu}{2}, \tag{24}$$

of the noise in the complex amplitudes. The corresponding noise in the optical power $P = |A|^2$ has the two-sided power density

$$S_{\delta P}(f) = \int_{-\infty}^{+\infty} G_{\delta P}(t)\;\mathrm{e}^{\mathrm{i}2\pi ft}\;\mathrm{d}t = \bar{P}\,h\nu, \tag{25}$$

with an average power $\bar{P}$, while the phase noise is characterized by

$$S_{\delta\varphi}(f) = \frac{h\nu}{4\bar{P}}. \tag{26}$$

The power noise given by (25) corresponds to the well-known shot-noise level.

Of course, the equations above can not be directly applied to the discrete amplitudes in the numerical model. For these, it is necessary to average the noise amplitudes over the time δt (which determines the temporal resolution). This results in a variance

$$\sigma^2_{\delta A}\big|_{\delta t} = \langle \delta A^*(t)\delta A(t)\rangle = \frac{1}{(\delta t)^2}\left\langle \int_0^{\delta t}\delta A^*(t)\,\mathrm{d}t \int_0^{\delta t}\delta A(t')\,\mathrm{d}t'\right\rangle$$
$$= \frac{1}{(\delta t)^2}\int_0^{\delta t}\int_0^{\delta t}\langle \delta A^*(t)\;\delta A(t')\rangle\,\mathrm{d}t\,\mathrm{d}t' = \frac{h\nu}{2\,\delta t}, \tag{27}$$

of the complex amplitude, or to variances of half this value in the real and imaginary parts. Similarly, in the frequency domain there is a variance $\frac{h\nu}{2\,\delta f}$ of the complex amplitudes. The initial pulse can be constructed by adding random values with e.g. a Gaussian distribution of the above calculated variance to the noiseless input values, which represent a Gaussian pulse shape.

During the pulse propagation, additional noise comes into play. Quantum noise influences result from spontaneous emission in the gain medium and from linear losses, while classical noise results from pump fluctuations and from fluctuations of the cavity length.

The noise from an ideal four-level gain medium with an intensity gain coefficient g, which is assumed to be $\ll 1$, can be described by adding complex noise amplitudes with the variance $\frac{h\nu}{2\,\delta t}g$ to the temporal amplitudes. For a large gain, the noise amplitudes can be added with the variance $\frac{h\nu}{2\delta t}\,(\exp(g)-1)$ after applying the noiseless gain. Three-level gain media (with reabsorption from the lower laser level) cause stronger noise, which can be described by introducing a factor $\theta > 1$ (as done in [2]).

Linear loss is also associated with added quantum noise; e.g., a linear loss with intensity loss coefficient l is related to complex temporal noise amplitudes with variance $\frac{h\nu}{2\,\delta t}l$. Nonlinear loss cannot be treated in this way. However, the nonlinear loss is often weak compared to the total loss, so that its noise influence can be introduced in an approximate way by adding quantum noise corresponding to a linear loss with the same average value.

As gain and loss should approximately balance each other near the steady state, one may apply twice the noise powers in the gain medium in order to incorporate the (equal) effect of losses. This has been done in the Haus/Mecozzi model [2]. However, the gain actually has a finite bandwidth while the losses may be broadband. This simplification is then a good approximation if the pulse spectrum is narrow compared to the gain bandwidth, which is the case in most (but not all) cases.

The action of the output coupler on the intracavity pulses is exactly the same as for any other linear loss. However, there is an important subtlety for the output pulses: the vacuum noise which enters the cavity through the output coupler is fully correlated with the vacuum noise reflected at the output coupler into the output beam. For a precise calculation of the quantum noise in the output, this effect would have to be taken into

account. However, the effect is only relevant for frequencies around the point where the plateau in the phase noise spectrum is reached, because only there the two noise contributions are comparable, so that their correlation matters.

3.5 *Classical noise*

In Sect. 3.3.1 the influence of classical excess pump noise has already been discussed. This should not be confused with quantum noise arising from gain (as discussed in Sect. 3.4) even for a noiseless pump mechanism.

Another important source of classical noise arises from mechanical vibrations of cavity mirrors. The main effect of these is a modulation of the cavity round-trip time, which causes timing jitter. It would be relatively easy to add such noise in the numerical model if the power density of the vibrations is known. However, such effects can also be handled by an analytical model, and so will not be considered further.

4 Numerical issues

4.1 *Numerical accuracy*

As described in Sect. 3.1.2, the temporal resolution δt is usually chosen so that the main part of the pulse is sampled by only ≈ 20 amplitudes. This means that the pulse maximum is not very precisely defined. Even if the position of the maximum is calculated by a second-order interpolation around the highest amplitude, the possible errors are much larger than the typical change of pulse position caused by quantum noise in a single cavity round-trip, which typically amounts to only to a few attoseconds. Therefore, particularly for long (picosecond) pulses it may seem surprising that such a course sampling of the pulses is sufficient to study timing jitter. However, there are solutions to this problem.

Firstly, to characterize the pulse position, the center of gravity can be used according to (1), which can be transformed into a form with simple sums for discrete amplitudes. This quantity, which depends on all amplitudes (not just on those near the peak), is much less influenced by numerical problems and at the same time represents a more realistic measure of the pulse position as measured by a photodetector which is typically too slow to resolve the details of the pulse shape.

An additional measure to obtain a high accuracy, very simply and effectively, is to artificially increase the noise powers by a large factor (e.g. 1000) and to rescale the resulting power spectra accordingly. As long as the fluctuations are still small enough, this does not adversely affect the results while making them much less sensitive to numerical errors.

4.2 *Limiting the number of cavity round-trips*

If the pulse data of M subsequent cavity round-trips for a laser with repetition rate f_{rep} is recorded , the noise spectra extending to the Nyquist frequency, $f_{\mathrm{rep}}/2$, can be calculated, while the lowest noise frequency is f_{rep}/M. This means that particularly for lasers with very high (multi-GHz) repetition rates, many round-trips have to be modeled for noise spectra extending down to reasonably low noise frequencies of 100 Hz, so that the computation time can become rather large.

Apart from optimizing the speed of the computations for a single round-trip, it is desirable to limit the number of required round-trips. The first and obvious measure is to study most phenomena for lasers with a reasonably low repetition rate of 100 MHz or less. Most of the insight gained in these situations can then be transferred to high repetition rate lasers. Another possible technique suitable for high repetition rate lasers is to combine several round-trips to one effective round-trip where all effects in the cavity (gain, loss, noise etc.) are correspondingly stronger. This is a valid approximation as long as all effects still stay sufficiently weak in each effective round-trip, so that the order in which the effects are applied does not matter. In multi-GHz solid-state lasers [20, 21], the actions of gain, loss, nonlinearity, and dispersion are indeed typically so weak that at least several round-trips can be combined, effectively speeding up the simulations by a factor of 5–10. In this way though, information on the highest noise frequencies is lost, however a simple extrapolation from lower noise frequencies is usually sufficient to compensate for this.

4.3 *Drifts of the pulse position*

In the numerical model, one should prevent the pulse position drifting toward the edges of the temporal range spanned by the set of complex amplitudes. A simple reason for this is that the calculation of the center of gravity pulse position (see Sect. 4.1) would have to be corrected if the pulse wrapped around the edges of the time trace. Another problem occurs for slow saturable absorbers, where the temporal evolution of the additional variable for the state of the absorber is not correctly calculated when wrap-around effects occur.

While the random walk of the pulse position caused by noise typically takes many round-trips until the pulse center has significantly changed, the edges of the temporal range can be reached much earlier by systematic drifts. Such drifts can be caused by a slow saturable absorber, which attenuates the leading part of the pulse more than the trailing part and thus shifts the pulse position. Once the drift rate has been calculated with the noise sources switched off, the drift can be numerically compensated for.

Even with compensated drifts, for longer simulated times it is necessary to limit the excursion of the pulse position from the center of the numerically represented region. The most reliable and simple technique is to regularly shift the whole time trace so that the peak of the pulse is near the center. One then has to sum up all applied shifts in order to obtain the correct timing positions for calculating the noise spectra.

4.4 *Starting with steady-state parameters*

The parameters of the initial pulse of the simulation runs should be close to those of the steady state. In simpler cases, one can start with analytically calculated parameters, obtained with equations from [22]. In other cases, one may have to approximate the steady state numerically, using many additional cavity round-trips before the actual simulation run.

5 Estimating spectral power densities

Once one has stored a sequence of timing errors for e.g. $2^{10} = 1024$, subsequent cavity round-trips, it appears triv-

ial to obtain a power spectrum of the timing fluctuations by applying a fast Fourier transform (FFT) to the data. However, significant problems can arise if the data are not handled with care.

It is well known [23] that before applying the FFT, the data should be multiplied with a so-called window function, which is zero at the ends of the time interval and non-zero in between. The reason for this is as follows. The power spectrum of the fluctuating signal which extends over an infinite range of time is required, but there is only data for a limited time interval. By Fourier transforming the data directly, this effectively yields the Fourier transform of the data multiplied with a step function, which is unity in the time interval and zero outside. This corresponds to convolution with a sinc function in the frequency domain, which does not only limit the spectral resolution, but also can spoil the resulting spectrum because of the relatively strong side lobes of the sinc function. By using one of several common window functions, one can strongly reduce the effect of such side lobes. In many applications, it does not matter which window function is chosen [23]; a common choice is the Welch window function, which is basically a second-order polynomial.

For the processing of timing errors of free-running (unstabilized) passively mode-locked lasers, the choice of window function is critical, and the Welch window is not a good choice. The reason is that the timing errors of such lasers does a random walk, i.e., drifts unbound for long observation times, which leads to a strong divergence of the spectral power density of the timing error at zero noise frequency. Such steep spectra are strongly affected by side lobes of window functions. Moreover, severe problems arise from the choice of a window function where the corresponding leakage function (basically the Fourier transform of the window function) has non-zero values for integer frequency offsets (i.e., for offsets which are integer multiples of δf). In this case, the diverging noise power near the zero frequency strongly affects the higher-frequency power values. This is exactly the case for the Welch window, which is therefore unsuitable for this application.

A first (but not always sufficient) remedy is to choose a window function where the corresponding leakage function has zeros at integer frequency offsets. This is the case for the Hanning window function, which is proportional to $1-\cos(2\pi t/T)$ when the time window ranges from $t=0$ to $t=T$. The Fourier transform of this is zero for frequencies j/T with integer values j and $|j|\geq 2$. As a result, even high power densities near $f=0$ have little effect on the higher-frequency power values, except for the first non-zero frequency. For a spectral power density proportional to f^{-2}, this leads to reasonable results when the first non-zero frequency value is discarded. However, for a spectral power density proportional to f^{-4}, the leakage problem is still unsolved.

The second remedy, to be used together with the first one, is to process the differences of subsequent timing errors instead of the timing errors themselves. These differences are related to changes of the instantaneous repetition frequency:

$$\delta f_{\mathrm{rep},n} = \delta\frac{1}{\bar{T}+(\delta t_n-\delta t_{n-1})} \approx -\frac{\delta t_n-\delta t_{n-1}}{\bar{T}^2}, \tag{28}$$

where $\bar{T}=1/f_{\mathrm{rep}}$ is the mean pulse period. Therefore, by Fourier transforming these timing differences (divided by $\bar{T}^2$), it is possible to obtain the spectral power density $S_{f_{\mathrm{rep}}}(f)$ of the instantaneous repetition frequency. From this, the power density of the phase noise can be calculated:

$$S_\varphi(f) = \frac{1}{f^2}S_{f_{\mathrm{rep}}}(f), \tag{29}$$

or for the timing noise,

$$S_{\Delta t}(f) = \left(\frac{\bar{T}}{2\pi}\right)^2 S_\varphi(f) = \left(\frac{1}{2\pi f_{\mathrm{rep}}}\right)^2 S_\varphi(f). \tag{30}$$

The first advantage of recording frequency noise rather than phase noise is that the resulting spectra become less steep. For example, with $S_\varphi(f)\propto f^{-2}$ there is a frequency-independent value of $S_{f_{\mathrm{rep}}}(f)$, where leakage problems do not occur. Even for $S_\varphi(f)\propto f^{-4}$, there is only $S_{f_{\mathrm{rep}}}(f)\propto f^{-2}$, where leakage problems can be minimized by using the Hanning window (see above). For even steeper phase noise spectra, problems could arise, and an even better window function would have to be used.

A second advantage of recording the frequency noise is that the drifts as discussed in Sect. 4.3, which correspond to a constant frequency offset, do not necessarily have to be removed before taking the Fourier transform.

Finally, the direct processing of phase noise leads to a 3 dB increase of the obtained noise power at the highest frequency values. This increase can be interpreted as an aliasing effect: noise components at frequencies above the Nyquist frequency are mirrored into lower frequency bins. This disturbing effect does not occur when processing frequency noise, because the frequency deviations are calculated from the differences of adjacent phase values, i.e., they are averaged over a finite time interval, and this effectively removes the frequency components above the Nyquist frequency.

For most other dynamical variables, such as the pulse energy or pulse duration, fluctuations only occur around the steady state, i.e., are bounded. In these cases, the power density at low frequencies stays finite, and the choice of a window function is not critical. Only for the optical phase noise, an unbounded random walk occurs, and a processing technique analogous to the one described above for the timing noise should be used.

The last issue to be considered is that the calculated noise power densities are fluctuating and approximate the real power densities only after averaging. Therefore, I typically do the numerical pulse propagation for four times as many pulses as required to obtain noise spectra down to the required minimum frequency. The simplest possibility would be to apply the FFT to subsequent arrays of simulated values. However, one obtains better averaging by applying the FFT to seven overlapping spans of data [23]. This nearly doubles the number of FFTs to be performed, but as the computation time is dominated by the pulse propagation and not by the FFT, this does not significantly increase the overall computation time, while the averaging is significantly improved.

6 Comparison of numerical and analytical results

For a comparison of the numerical results with those from the analytical Haus/Mecozzi model [2], a simple situation must be chosen which can be handled by the analytical model. I used the following parameters for a soliton mode-locked laser operating at 1064 nm, repetition rate $f_{\mathrm{rep}} = 100\,\mathrm{MHz}$, output coupler transmission 5%, average output power 100 mW, gain bandwidth 20 nm (with a Gaussian shaped gain spectrum), an absorber with 0.5% unsaturated power absorption (operated so that the peak power is twice the saturation power), intracavity dispersion $3000\,\mathrm{fs}^2$ per round-trip, Kerr nonlinearity 10^{-6} rad/W, leading to soliton pulses with 0.53 ps duration and 33 mrad nonlinear peak phase shift per round-trip.

The gain saturation was assumed to depend only on the pulse energy (not on its history) as in the analytical model. The assumptions for both models are in effect identical, expect for small details such as the shape of the gain spectrum (Gaussian for the numerical model and parabolic for the analytical model), and the frequency dependence of the spontaneous emission noise, which is taken into account only in the numerical model.

Originally, there was a 3-dB discrepancy between numerical and analytical results at high noise frequencies. I found, however, that (54)–(57) in [2] for the diffusion constants are incorrect. Only (56) has been corrected in the erratum [24], but the other terms should be smaller by a factor of 2. Starting with (26)–(29) and (44) in [2], one arrives at the following corrected results (using the notation of [2]):

$$D_w = 2w_0\theta\frac{2g}{T_{\mathrm{R}}}h\nu\,, \tag{31}$$

$$D_\theta = \frac{2}{3w_0}\left(1+\frac{\pi^2}{12}\right)\theta\frac{2g}{T_{\mathrm{R}}}h\nu\,, \tag{32}$$

$$D_p = \frac{2}{3w_0\tau^2}\theta\frac{2g}{T_{\mathrm{R}}}h\nu\,, \tag{33}$$

$$D_t = \frac{\pi^2\tau^2}{6w_0}\theta\frac{2g}{T_{\mathrm{R}}}h\nu\,. \tag{34}$$

In particular, the value of D_t was too high by a factor of 2, causing the 3-dB discrepancy. Note that the errors in the diffusion constants have also propagated into later articles [3].

From the diffusion constants, the noise spectra can be calculated. In particular, for the timing noise, the two-sided spectral power density (adapted to this work's notation) was found to be

$$S_{\Delta t}(f) = \frac{D^2}{T_{\mathrm{rt}}^2}\frac{D_p}{(2\pi f)^2\left((2\pi f)^2+\tau_p^{-2}\right)} + \frac{D_t}{(2\pi f)^2}, \tag{35}$$

where D is the group delay dispersion per round-trip and

$$\tau_p = \frac{3\pi^2\,T_{\mathrm{rt}}\,\Delta f_{\mathrm{g}}^2\,\tau^2}{2g}, \tag{36}$$

with Δf_{g} being the FWHM gain bandwidth, τ the FWHM pulse duration divided by 1.763, and g the saturated intensity gain per round-trip.

With the corrected diffusion constants, the analytical and numerical results are fully consistent, as shown in Fig. 1. Here and in all subsequent spectra the vertical axis shows $10\log\left(S_\varphi(f)1\,\mathrm{Hz}\right)$ in dBc/Hz, rather than directly as $S_\varphi(f)$ in $\mathrm{rad}^2/\mathrm{Hz}$. This convention leads to more readable graphs and has often been used in the literature. As shown in Sect. 2, for small phase excursions the obtained values indeed indicate the noise level in the photodiode signal relative to the peak at $f = f_{\mathrm{rep}}$, which justifies the units dBc/Hz. The black points in Fig. 1 indicate the numerically calculated timing noise power densities for the intracavity pulses, which on average agree with the analytically calculated values (solid line). For the output pulses (gray points), the phase noise approaches a constant level at high frequencies. This is due to zero-point quantum fluctuations (vacuum noise) reflected at the output coupler mirror [25]. The plateau set by these fluctuations represents the fundamental quantum limit for the timing jitter (see part II).

As the Haus/Mecozzi model [2] is based on soliton perturbation theory, with the assumption that the absorber action is weak compared to the actions of dispersion and nonlinearity, one might not expect it to be valid for a case without any dispersion and nonlinearity. However, Fig. 2 shows that even in this case the analytical and numerical results agree with each other, and the analytical results are apparently correct. Closer inspection of this situation reveals that the two mechanisms by which quantum noise causes timing jitter are actually not at all related to the mechanism which shapes the sech^2 pulses. While this pulse shape can arise from soliton effects, it can also approximately arise from the action of a fast or slow saturable absorber. In any case, two mechanisms allow the quantum noise from spontaneous emission to affect the timing of the pulses. The direct mechanism involves a random shift of the pulse position by spontaneous emission. As the second mechanism, spontaneous emission causes fluctuations of the center frequency, which translate into changes of group velocity in the presence of dispersion, so that the pulse timing also fluctuates. Because the translation from group velocity changes, into timing errors involves an integration, an additional factor f^{-2} is obtained for this part of the spectral power density of the timing noise. These

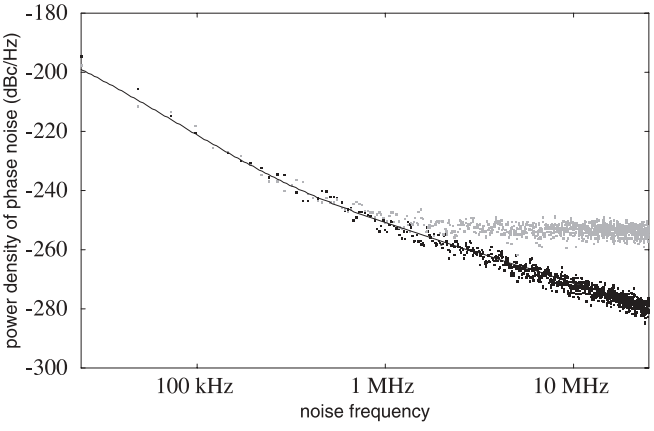

FIGURE 1 Timing phase noise spectra for a hypothetical soliton mode-locked laser with a fast saturable absorber. *Solid line*: result of analytical model. *Black points*: result of numerical model for the intracavity pulses. *Gray points*: numerical result for the output pulses. The vertical axis displays $10\times\log\left(S_\varphi(f)\times 1\,\mathrm{Hz}\right)$

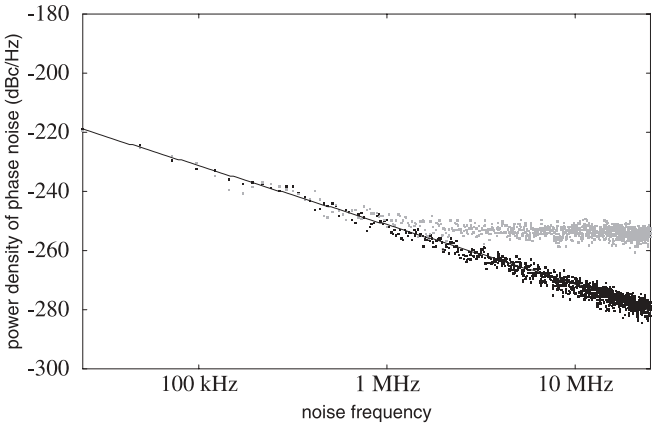

FIGURE 2 Timing phase noise spectra for a hypothetical mode-locked laser with a fast saturable absorber but no dispersion and no Kerr nonlinearity. *Solid line*: result of analytical model. *Black points*: result of numerical model for the intracavity pulses. *Gray points*: numerical result for the output pulses

mechanisms have been identified in [2], but it was not recognized that they do not depend on a soliton pulse-shaping mechanism.

7 Conclusions

I have described in detail a numerical model which can be used to simulate various kinds of noise, in particular the timing noise, of mode-locked lasers. Although the general approach is straight-forward, a number of issues have to be observed and appropriately treated in order to obtain reliable results. A comparison with an earlier analytical model for simple cases showed perfect agreement of the results after correcting some trivial errors in the analytical calculations.

The numerical approach is most flexible, allowing treatment of actively or passively mode-locked lasers and includes effects like realistic gain saturation, higher-order dispersion, or various nonlinearities. Part two of this paper [6] will present a comprehensive discussion of the noise of mode-locked lasers, based both on the numerical model described here and on analytical results.

ACKNOWLEDGEMENTS The author is grateful to Ursula Keller for stimulating this work, and to G.J. Spühler for making useful comments on the manuscript.

REFERENCES

1 D.R. Hjelme, A.R. Mickelson: IEEE J. Quant. Elect. **QE-28**, 1594 (1992)
2 H.A. Haus, A. Mecozzi: IEEE J. Quant. Elect. **QE-29**, 983 (1993)
3 L.A. Jiang, M.E. Grein, H.A. Haus, E.P. Ippen: IEEE J. Sel. Top. Quant. Elect. **QE-7**, 159 (2001)
4 U. Keller, D.A.B. Miller, G.D. Boyd, T.H. Chiu, J.F. Ferguson, M.T. Asom: Opt. Lett. **17**, 505 (1992)
5 U. Keller, K.J. Weingarten, F.X. Kärtner, D. Kopf, B. Braun, I.D. Jung, R. Fluck, C. Hönninger, N. Matuschek, J. Aus der Au: IEEE J. Sel. Top. Quant. Elect. **2**, 435 (1996)
6 R. Paschotta: Appl. Phys. B DOI 10.1007/s00340-004-1548-9 (2004)
7 A. Braun, V. Khalfin, J. Abeles, C. DePriest, E. Park, P. Delfyett: In: Conf. Lasers Electro-optics (CLEO), (Opt. Soc. Am.), talk CMS2, 2001
8 D. v. d. Linde: Appl. Phys. B **39**, 201 (1986)
9 I.G. Fuss: IEEE J. Quant. Elect. **QE-30**, 2707 (1994)
10 D. Eliyahu, R.A. Salvatore, A. Yariv: J. Opt. Soc. Am. B **13**, 1619 (1996)
11 D. Eliyahu, R.A. Salvatore, A. Yariv: J. Opt. Soc. Am. B **14**, 167 (1997)
12 E.S. Ferre-Pikal, J.R. Vig, J.C. Camparo, L.S. Cutler, L. Maleki, W.J. Riley, S.R. Stein, C. Thomas, F.L. Walls, J.D. White: in IEEE Int. Freq. Control Symp., 1997
13 D.C. Hutchings, M. Sheik-Bahae, D.J. Hagan, E. W. van Stryland: Optical Quant. Elect. **24**, 1 (1992)
14 C.C. Harb, T.C. Ralph, E.H. Huntington, D.E. McClelland, H.A. Bachor: J. Opt. Soc. Am. B **14**, 2936 (1997)
15 C.H. Henry: IEEE J. Quant. Elect. **QE-18**, 259 (1982)
16 F. Salin, J. Squier, M. Piché: Opt. Lett. **16**, 1674 (1991)
17 G.P. Agrawal: Nonlinear Fiber Optics (Academic Press, 1989)
18 G.P. Agrawal: Nonlinear Fiber Optics (Academic Press, San Diego, CA, 2001)
19 P.D. Drummond, J.F. Corney: J. Opt. Soc. Am. B **18**, 139 (2001)
20 L. Krainer, R. Paschotta, S. Lecomte, M. Moser, K.J. Weingarten, U. Keller: IEEE J. Quant. Elect. **QE-38**, 1331 (2002)
21 L. Krainer, R. Paschotta, G.J. Spühler, I. Klimov, C.Y. Teisset, K.J. Weingarten, U. Keller: Electron. Lett. **38**, 225 (2002)
22 R. Paschotta, U. Keller: Appl. Phys. B **73**, 653 (2001)
23 W.H. Press, B.P. Flannery, S.A. Teukolsky, W.T. Vetterling: *Numerical recipes in Pascal* (Cambridge Uni. Press, 1992)
24 H.A. Haus, A. Mecozzi: IEEE J. Quant. Elect. **QE-30**, 1966 (1994)
25 H.A. Haus, M. Margalit, C.X. Yu: J. Opt. Soc. Am. B **17**, 1240 (2000)